Journal of Solid State Chemistry 183 (2010) 1423–1432

Contents lists available at ScienceDirect

Journal of Solid State Chemistry

journal homepage: www.elsevier.com/locate/jssc

Template-free synthesis of CdS hollow nanospheres based on an ionic liquid assisted hydrothermal process and their application in photocatalysis

Xinping Li, Yanan Gao, Li Yu, Liqiang Zheng *

Key Laboratory of Colloid and Interface Chemistry, Shandong University, Ministry of Education, Jinan, Shandong 250100, People's Republic of China

ARTICLE INFO

Article history:
Received 2 January 2010
Received in revised form
23 February 2010
Accepted 4 April 2010
Available online 21 April 2010

Keywords:
CdS
Hollow nanospheres
Ionic liquid
Mechanism
Photocatalysis

ABSTRACT

Polycrystalline CdS hollow nanospheres with diameter of about 130 nm have been successfully synthesized in high yield by an ionic liquid (IL) assisted template-free hydrothermal method for the first time. Both the molar ratios of Cd/S precursor in the solution and the reaction temperature play important roles in the formation of the CdS hollow nanospheres. The concentrations of capping agent hexamethylenetetramine (HMT) and polyvinylpyrrolidone (PVP) are also crucial for the morphology and size of the final product. IL was found to be a key component in the formation of CdS hollow structures, because solid spheres were obtained in the absence of IL. A subsequent growth mechanism of hollow interior by localized Ostwald ripening process has been further discussed. Such hollow structures show high photocatalytic ability in the photodegradation of methylene blue.

1. Introduction

Hollow-structured materials have attracted much attention due to their widespread applications in many fields, such as catalysis, drug delivery, photo devices, lightweight fillers, acoustic insulators and so on [1,2]. Among all the methods employed for preparing hollow structures, hard templates such as polymers, inorganic nanospheres and soft templates such as micelles, oil droplets and gas bubbles have been commonly used [3,4]. However, synthesis with hard templates requires eliminating the cores via chemical etching, calcination, or optical excavation which is complicated and energy consuming. Soft templates are relatively easy to remove yet the morphology and monodispersity are generally difficult to control [1–6]. Recently, many efforts have been devoted to develop template-free methods in order to avoid complex processes [5,7]. However, great challenges still remain to obtain pure and size-controllable hollow structures.

As a common semiconductor material, transition-metal chalcogenides have attracted much attention due to their excellent properties and wide-ranging potential applications [8,9]. In particular, CdS, as an important semiconductor of II–VI group with a band gap at 2.42 eV at 300 K, is of great interest due to its important applications as nanoelectronic and optoelectronic materials [10–13]. Since the material properties mainly depend on the morphological features, a variety of CdS nanostructures have been synthesized, including nanowires [10], nanoribbons [11], nanobelts [12] and hierarchical dendrites [13]. Many efforts have been devoted to the synthesis of CdS hollow micro- and nanostructures. So far, the synthesis of CdS hollow micro- and nanostructures has been made mainly on the base of soft templates [14–17]. For example, Xie and co-workers [14] have synthesized CdS hollow spheres via a source–template-interface route in solution with CS_2 oil droplets as template. Qian and co-workers [15] prepared octahedral CdS hollow microcages on the base of the ion interface reaction process by using $CdMoO_4$ crystals as in situ sacrificial templates. Recently, hollow CdS nanoboxes, having paper-thin walls of well-defined facts, have been firstly synthesized at 170 °C via a simple reaction using Na_2SeO_3 as interior quasitemplates and ethylenediamine as exterior molecular templates. Unlike conventional templates Na_2SeO_3 can be easily and thoroughly washed off with water after the reaction [16]. Interestingly, it was reported that CdS hollow spheres can be prepared by reacting thiourea and cadmium acetate using a one-step method without any template and external wave field [18]. However, to our knowledge, there is still a need to develop a more straightforward procedure for fabricating CdS hollow structures with controlled shapes in an effective and reproducible fashion.

Recently, ionic liquids (ILs), as a class of environmentally benign solvents, have shown great interest in various fields, such as biphasic reactions, chemical synthesis, electrochemistry, catalysis, liquid–liquid separations and interfacial synthesis [19,6,17]. The physicochemical properties of ILs can be changed by selecting the appropriate combination of cations and anions. In

* Corresponding author. Fax: +86 531 8836 4750.
E-mail address: lqzheng@sdu.edu.cn (L. Zheng).

0022-4596/$ - see front matter © 2010 Elsevier Inc. All rights reserved.
doi:10.1016/j.jssc.2010.04.001

particular, the 1-alkyl-3-methyl-imidazolium types of ILs combined with specific anions are known to self-organize in a way that is adaptable to the fabrication of metal nanostructures [20]. Novel nanostructures can be produced by choosing suitable ILs system. TiO_2 hollow microspheres have been prepared in 1-butyl-3-methylimidazolium hexafluorophosphate ([bmim][PF_6]), and the size of products can be affected by physical conditions such as stirring rate and temperature [6]. CoPt nanorods have been synthesized in 1-butyl-3-methylimidazolium-bis(trifluoromethylsulfonyl)imide ([bmim][Tf_2N]) [20]. However, to our knowledge, there has not been any report for the synthesis of CdS hollow spheres in the presence of ILs. In addition, the controlled construction of well-defined hollow structures with a simple method is still a challenge.

Herein, we report the synthesis of CdS nanometer-sized hollow spheres by a very simple one-step hydrothermal method in the presence of water-immiscible IL, [bmim][PF_6]. This is the first report for the ILs assisted formation of CdS hollow nanospheres. The as-prepared CdS hollow nanospheres have an average diameter of about 130 nm and the shells were constructed with small particles. To elucidate the formation mechanism, the effects of variations of reaction conditions, including molar ratio of cadmium precursor to sulfide precursor (abbreviated as Cd/S), reaction temperature, the concentration of capping agents and reaction time on the products have been investigated. The possible formation mechanism of hollow CdS nanoparticles is proposed. A new and attractive application of CdS hollow nanospheres is photocatalysis, and they show higher photocatalytic efficiency in the degradation of methylene blue (MB).

2. Experimental section

2.1. Chemicals and synthesis

$CdCl_2$ was obtained from Hengxin Chemical Reagents Co. Ltd. China. Polyvinylpyrrolidone (PVP) was provided by ISP TECHNOLOGIES INC. Hexamethylenetetramine (HMT) was purchased from Tianjin Guangcheng Chemical Reagents Co. Ltd. China and thioacetamide (TAA) is a product of Sinopharm Chemical Reagents Co. Ltd. China. All chemicals were of analytical grade and used without further purification. The IL, [bmim][PF_6], was synthesized according to the literature [21]. Double distilled water was used in all experiments.

In a typical procedure, 0.3 mmol $CdCl_2$, 0.12 g PVP (K30; Mw ≈ 50,000) and 0.6 mmol HMT were dissolved into 1 mL deionized water to form a clear solution, then 1 mL [bmim][PF_6] was added into the solution and vigorously stirred for 10 min. After that, TAA solution (3 mL; 0.6 mmol in water) was dropped into the above mixture. After stirring for 30 min, the solution was transferred into a 10 mL Teflon-lined stainless steel autoclave, sealed and maintained at 150 °C for 24 h in an electric oven. The autoclave was then cooled to room temperature naturally. The product was collected by centrifugation and washed several times with distilled water and absolute ethanol. Finally the product was dried in a vacuum oven at 60 °C for 5 h. The yellow product was collected for further characterization. The different experimental condition was performed when studying their effects on the final products but the other conditions were kept the same.

2.2. Photocatalysis

The photodegradation activity of the as-prepared CdS hollow nanospheres was measured using a methylene blue (MB) solution with concentration of 3×10^{-5} M, and 0.05 g sample was dispersed into a column-like container containing 200 ml MB solution by magnetic stirring. Prior to irradiation, the solution was stirred under dark conditions for 30 min, in order to establish an adsorption–desorption equilibrium. We used a 125 W high-pressure mercury lamp (λ=320–400 nm, λ_{max}=365 nm) for the UV light to test the photocatalytic activity. At certain irradiation intervals, aliquots of about 3 ml solution were withdrawn from the suspension and then centrifuged. The photocatalytic performance of the sample was subsequently gauged by measuring intensity changes of the optical absorbance peaks at 664 nm, of aqueous supernatant aliquots containing MB, using a UV–vis spectrophotometer (Lambda 35, Perkin-Elmer).

2.3. Characterization

The crystal structures of the CdS powder were characterized by X-ray scattering (XRD; D8 Advance X-ray Diffractometer) using Cu$K\alpha$ radiation source (40 kV) over a range of 2θ angles from 10° to 80°. SEM images were taken to measure the sizes and morphologies of CdS materials by using a field emission scanning electron microscope (JEOL JSM-7600F) operating at 3.0 kV. The morphology and structure of the synthesized materials were also studied using transmission electron microscope (TEM; JEM-100CXII (JEOL)) at an opening voltage of 80 kV and high resolution transmission electron microscopy (HRTEM; JEM-2100) with an accelerating voltage of 200 kV. Nitrogen absorption and desorption measurements were performed on a QuadraSob SI apparatus. The surface areas were calculated by the Brunauer–Emmett–Teller (BET) method, and the pore size distribution was calculated from the adsorption isotherm curves using Brunauer–Joyner–Halenda (BJH) method. The ultraviolet–visible (UV–vis) absorption spectrum was recorded on a HITACHI U-4100. The photoluminescence (PL) spectrum was measured on an LS-55 fluorescence spectrophotometer. Raman spectrum was obtained on solid samples placed onto a glass wafer. Spectra were measured on a LabRAM HR 800 Raman microscope with 473 nm laser for excitation.

3. Results and discussion

3.1. Structural characterization of CdS hollow nanospheres

Throughout our experiments, the optimal conditions for the formation of CdS hollow nanospheres are 150 °C for the reaction temperature, 0.06 mmol for the HMT and 0.12 g for the PVP, 1:2 for the molar ratio of Cd/S precursor and 24 h for the reaction time. The purity and crystallinity of CdS hollow nanosphere were examined using XRD. Fig. 1 shows the XRD patterns of the as-prepared CdS hollow nanospheres by the [bmim][PF_6] assisted hydrothermal method. All the diffraction peaks can be indexed to hexagonal phase of CdS crystal (JCPDS card 41-1049). Additionally, no peaks of impurities were detected, indicating the high purity of the product.

Fig. 2 shows the typical SEM and TEM images of the hollow nanospheres. From SEM images it can be seen that these hollow nanospheres are nearly homogeneous with diameter of about 130 nm. It is found that each hollow nanosphere is composed of some smaller particles. The hollow nature of the nanosphere is clearly depicted via the partially opened nanospheres (Fig. 2B). A more clear evidence of the hollow structure can be found from the TEM image. As demonstrated in Fig. 2C, there is a strong contrast difference in all of the nanospheres with a pale center and relatively dark edge, confirming the hollow structure.

Furthermore, these hollow nanospheres are nearly monodisperse and the shell consists of small nanocrystallites with their sizes ranging from 20 to 35 nm, which is in accordance with the XRD and SEM results. The corresponding energy-dispersive X-ray spectrum (EDS) (Fig. 2D) further indicates that the products consist of S and Cd with a ratio of 1:1, which is consistent with the stoichiometric CdS. The morphology of CdS hollow nanospheres was further analyzed by HRTEM. Fig. 3A shows the TEM image of a single CdS hollow nanosphere, and Fig. 3B and C shows the HRTEM images of different space corresponding to the square and rectangle parts in Fig. 3A. Different crystal orientations can be observed in the same hollow nanosphere. As shown in Fig. 3B, C, the observed lattice plane spacing calculated from HRTEM images is 0.31 and 0.35 nm, which corresponds to the spacing length of the (1 0 1) and the (1 0 0) planes of hexagonal CdS structures, respectively. The HRTEM pattern also indicates that the hollow nanospheres are composed of smaller nanocrystals. The pattern of selected area electron diffraction (SAED) of a single CdS hollow nanosphere further indicates the polycrystalline nature of the CdS hollow nanospheres.

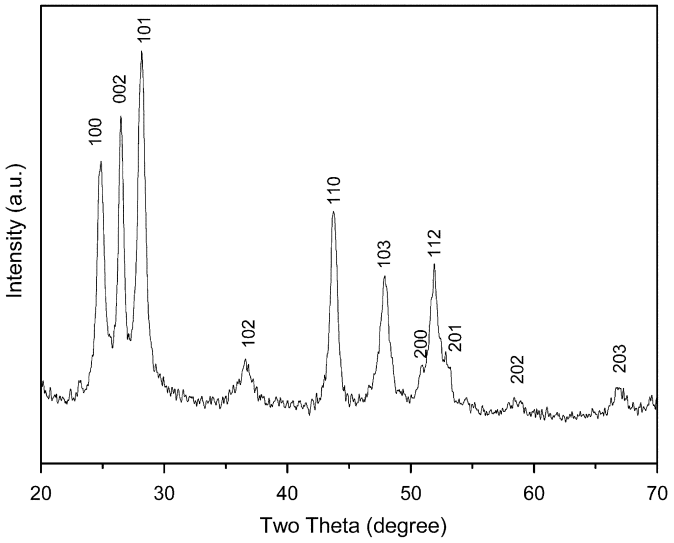

Fig. 1. XRD patterns of the CdS hollow nanospheres.

On the basis of the above discussion, CdS hollow nanospheres constructed by sub-crystallites should have a large quantity of pores in the shells. To investigate the porous structure of the hollow nanospheres, N_2 adsorption–desorption isotherm and Brunauer–Emmett–Teller (BET) plot were obtained (Fig. S1). The pore size distribution plot (insert in Fig. S1) shows that the pore size was in the range of 2–46 nm, and most pores are distributed in the range of 5–15 nm. The specific surface area (S_{BET}) of CdS hollow nanospheres calculated using the BET equation is 31.40 m^2/g. The formation of mesoporous structure is attributed to the aggregation of small crystallites in the shell wall of hollow nanospheres, which is consistent with TEM images.

3.2. Factors influencing the formation of the CdS hollow nanospheres

Both the molar ratios of Cd/S precursor in the solution and the reaction temperature play important roles in formation of the CdS hollow nanospheres. In addition, the concentrations of capping agent (HMT, PVP) are also crucial for the morphology and size of the final product.

3.2.1. Effect of different ratios of Cd/S on the morphology of CdS hollow nanospheres

The morphology of the CdS hollow nanospheres varied by changing the molar ratio of Cd/S. Fig. 4 shows the TEM images of the sample prepared with different Cd/S molar ratios of 2:1, 1:1, 1:3 and 1:4. In all cases, the concentration of S precursor was fixed (0.06 mmol). When the molar ratio of Cd/S is 2:1 (Fig. 4A), it

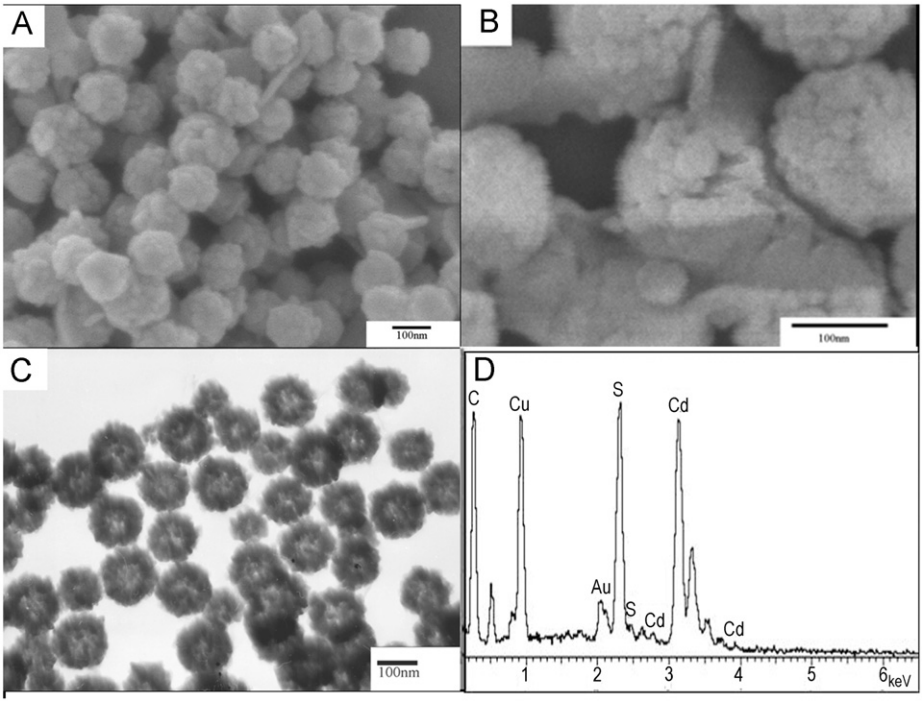

Fig. 2. SEM and TEM images of the typical as-prepared CdS hollow nanospheres: (A) low- and (B) high-magnification SEM images of hollow nanospheres, (C) TEM image of CdS hollow nanospheres and (D) EDS spectrum of the corresponding sample.

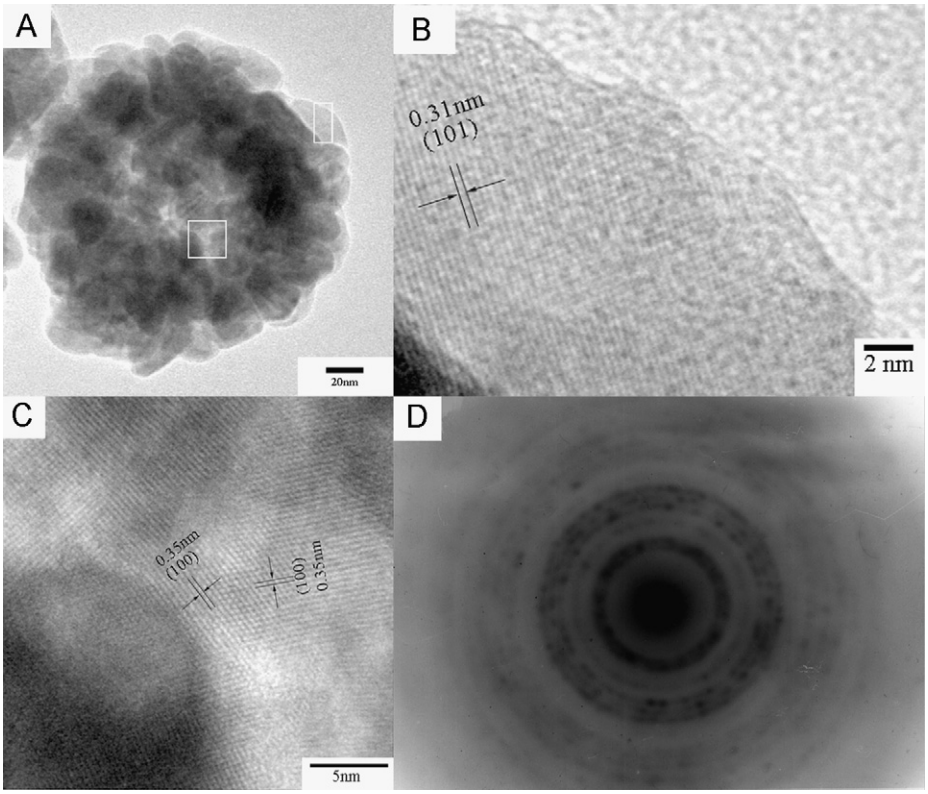

Fig. 3. TEM and SAED patterns of a single CdS hollow nanosphere: (A) TEM image of an individual CdS hollow nanosphere, (B) HRTEM image corresponding to the rectangle part in (A), (C) HRTEM image of the space corresponding to the square part in (A) and (D) SAED patterns of hollow structures.

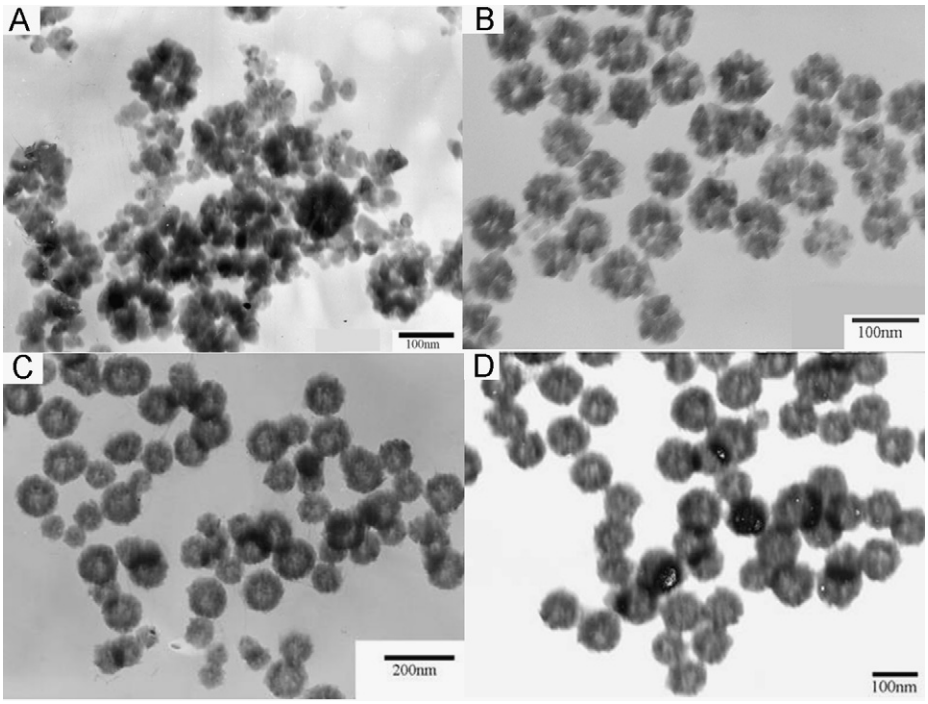

Fig. 4. TEM images of samples prepared at different Cd/S molar ratio. In all cases, the concentration of S precursor was fixed. (A) 2:1, (B) 1:1, (C) 1:3 and (D) 1:4.

can be clearly seen that plenty of random aggregated nanocrystallites coexist with few hollow nanospheres, which consist of smaller nanocrystallites that assembled incompactly together. When the molar ratio of Cd/S is 1:1 (Fig. 4B), the CdS nanocrystallites aggregate to form sphere-like hollow structure with a diameter of about 70 nm, accompanied by a few smaller nanoparticles. By increasing the molar ratio of Cd/S to 1:2 (Fig. 2C), nearly monodispersed hollow nanospheres with a larger diameter of ca. 130 nm were formed; it is interesting to find that small particles almost disappeared. The morphology of

the hollow CdS nanospheres did not change obviously any more with further increasing the molar ratio of Cd/S from 1:3 to 1:4, as can be seen in Fig. 4C and D, except that the shell of the particles becomes more compact and the hollow interior is not so obvious from the TEM images. It is well known that the process of crystal growth can be divided into two steps: an initial nucleation stage and a subsequent crystal growth stage, both of which can be influenced by the original reactant ratio [22]. When the Cd/S ratio is increased, the initiative free Cd^{2+} concentration in the solution increases; therefore, the nucleation speed is fast, which leads to a faster depletion of precursors. As a result, the crystal growth speed was decreased and the nuclei grow into deformed aggregated nanocrystallites with small particles. While the Cd/S ratio is decreased, the lower free Cd^{2+} concentration leads to a slower nucleation speed and a faster growth speed, which is favorable for the nuclei growth process. So small particles disappear and the nuclei grow into larger hollow nanospheres. All results suggested that the morphology and size of the product are dependent on the initial Cd/S molar ratios.

3.2.2. *Effect of reaction temperature on the growth of CdS nanocrystals*

The influence of reaction temperature on the formation of the CdS nanostructures was also studied. Fig. 5 shows the TEM images of CdS structures prepared at different reaction temperatures. No CdS hollow structure was found at 85 °C; only solid spheres (50–100 nm) were observed, as shown in Fig. 5A. When the temperature is increased to 100 °C, larger solid spheres with average diameter of 100 nm were obtained (Fig. 5B). Hollow nanospheres with a diameter of ca. 150 nm were formed when the temperature is increased to 180 °C; it is obvious that the morphology of the hollow structures is not perfect. From this result, we can deduce that with the increasing temperature, the ionic transportation is fast and thus large number of crystal nuclei would be formed, which is favorable for the aggregation of CdS nanocrystals. So, large-sized CdS hollow nanospheres can be obtained at high temperatures. However, at high temperature like 180 °C, the capping agents on the surfaces of CdS crystal can be weakened, thus the CdS crystal has a relatively faster growth rate, which results in the imperfectly hollow structure [22]. All the results indicate that during the synthesis of CdS nanocrystals, temperature is also of importance in the formation of hollow structures CdS nanocrystals.

3.2.3. *Effects of HMT, PVP and IL ([bmim][PF_6]) on the CdS hollow nanospheres*

We have shown that CdS hollow nanospheres can be obtained in high yield under suitable experimental conditions (150 °C, PVP=0.12 g, HMT=0.6 mmol, 24 h). It is known that capping agents are very important to control the morphology and size of materials. So, the effects of PVP and HMT concentrations on CdS nanostructures were also studied. When PVP was absent, no hollow nanospheres were obtained (Fig. 6A), but irregular-shaped CdS aggregates instead. Only polyhedron (30–50 nm) was observed without HMT (Fig. 6B). Therefore, both PVP and HMT certainly played important roles in shaping the CdS hollow nanospheres. However, it is necessary to note that, the PVP concentration in the solution has a slight impact on the morphology of CdS hollow structures (Figure S2 A, B, Supporting Information). In addition, we further investigated the effect of HMT concentration on the morphology of the product, which was frequently used as a capping agent in the hydrothermal synthesis of ZnO nanocrystals [23–25]. In this attempt, the concentration of PVP was fixed at an optimal value, namely, 0.12 g. Fig. 7A–C shows the CdS morphology evolution with the increasing concentration

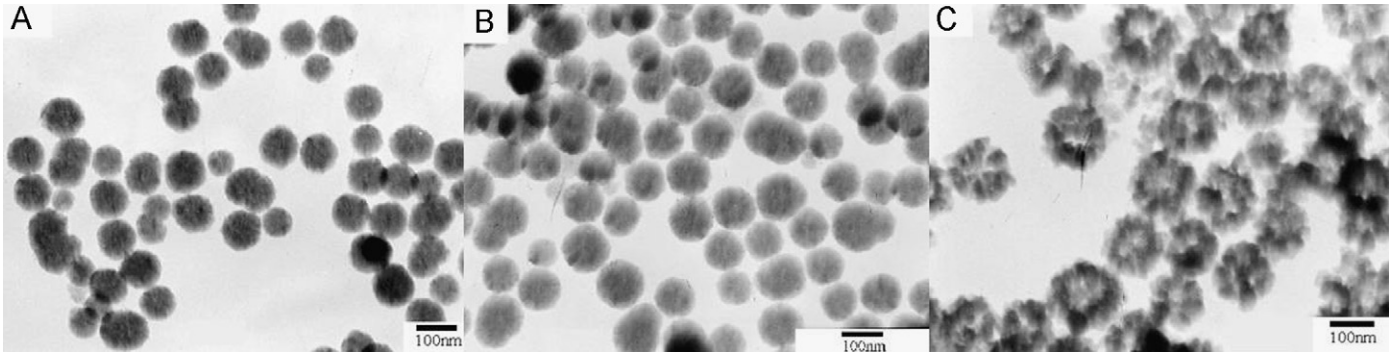

Fig. 5. TEM images of the as-prepared CdS nanostructures at different reaction temperatures. (A) 85, (B) 100 and (C) 180 °C.

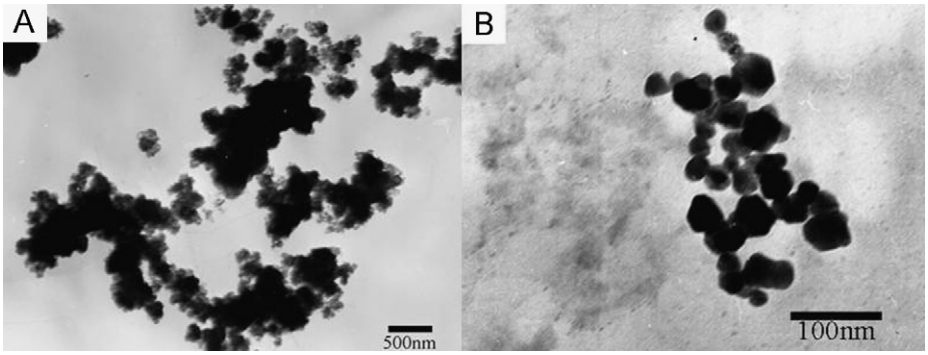

Fig. 6. TEM images of the CdS nanostructures prepared in the absence of (A) PVP and (B) HMT.

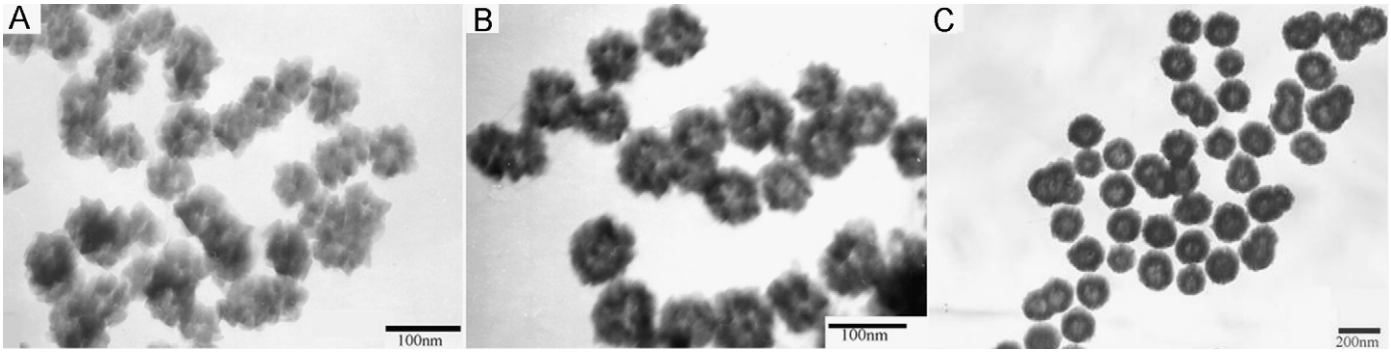

Fig. 7. (A–C) are the shape evolutions of CdS structures with different amounts of HMT: (A) 0.1, (B) 0.3 and (C) 1.2 mmol.

of HMT in the hydrothermal process. At a lower concentration (0.1 mmol), it was found that deformed hollow structures were observed with irregular shape, each consists of assembled small crystallites (Fig. 7A). By increasing the concentration of HMT to 0.3 mmol, approximately sphere-like hollow structures with a diameter of 70 nm were formed (Fig. 7B); we can see that the hollow interior was not obvious. Sphere-like hollow nanostructures with good monodisperse were formed when the concentration of HMT reached 0.6 mmol (Fig. 2C), as mentioned above, the diameter of hollow nanospheres was about 130 nm. However, if the concentration of HMT was increased to 1.2 mmol, hollow nanospheres with a diameter of ca. 170 nm were formed (Fig. 7C). The results show that HMT also played an important role in the formation of CdS hollow nanostructures. On increasing the concentration of HMT, the size of the obtained hollow nanospheres becomes larger and the shell becomes smooth and compact. This implies that HMT induced the aggregation of CdS nanocrystallites with sphere-like structure. A similar role of HMT in our experiment has been reported by Chen's group [25], in which HMT was used to prepare 3D CdS nanocrystals with flower-like structure. It was proposed that HMT could selectively adsorb on certain faces of CdS seeds for its binding capacity. From these phenomena, we speculate that at the initial stage, PVP may cap or adhere selectively to peculiar surfaces of amorphous CdS nanocrystallites and controlled their growth. Simultaneously, HMT could form complex compounds with bivalent ions. The lone-pair involved nitrogen atoms of HMT molecules can selectively bind or be adsorbed on certain faces of the CdS seeds to influence the growth of these faces and the aggregation of small nanoparticles, which led to a smooth shell of solid nanospheres of CdS that favors the subsequent formation of CdS hollow nanospheres [23–25]. Thus, we can see that both HMT and PVP are indispensable for the formation of perfect CdS hollow nanospheres.

To elucidate the role of [bmim][PF_6] in the formation process of CdS hollow nanospheres, a comparative experiment process was carried out in the absence of [bmim][PF_6]. A typical TEM image in Fig. 8 reveals that no hollow structures are found without [bmim][PF_6], except some solid spheres. This indicates that IL also played a key role in determining the hollow structure of the product. Furthermore, we found that the concentration of [bmim][PF_6] has no obvious effect on the morphology of final product, which means that [bmim][PF_6] is not used as a template in the experiment. The unique role for IL in the synthesis of CdS hollow nanospheres may be ascribed to the special properties of IL [bmim][PF_6], which is essentially molten salt and immiscible with water to a large extent. During the reaction process, the IL [bmim][PF_6] located in the lower phase due to its higher density than water and the reaction would take place in the above water phase. When small CdS nanoparticles were formed in water phase, the CdS precipitate would go down into the [bmim][PF_6] phase, which blocked the fast growth of CdS. In this case, the product of CdS is loose that favors the formation of hollow nanospheres [26,27]. Furthermore, compared our results with Xu's work [18], which was the first report for the synthesis of CdS hollow nanospheres with a template-free method, we can see that, in the presence of ionic liquid, the hollow structure could be formed with a much more lower molar ratio of S/Cd. So we deduced that IL [bmim][PF_6] may promote the mass transport during the reaction process, which in turn accelerated the formation process of hollow structures. It is the first time to prepare sulfide hollow nanospheres with an IL assisted hydrothermal method, although the explicit function of IL is not clear at this moment, it can be seen that [bmim][PF_6] plays an important role in our experiment.

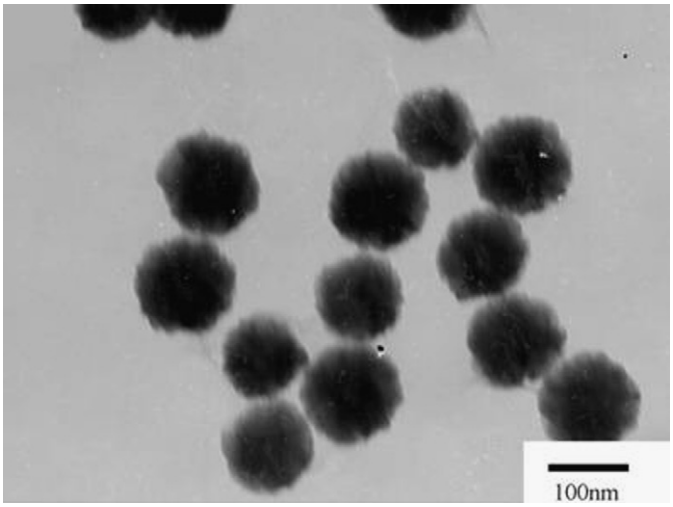

Fig. 8. TEM image of the products prepared without [bmim][PF_6].

Furthermore, we carried out comparative time-dependent experiments during the process to investigate the effect of HMT, PVP and IL. Fig. S3 shows the morphology transformation at different reaction time of 0.5, 7 h, respectively. Fig. S3 A, B is the TEM image of the product obtained in the absence of HMT at 0.5 and 7 h. It was found that at the initial stage, we obtained 50 nm sphere like nanocrystals, which then grew into irregular aggregates consisting of smaller particles at 7 h; finally, polyhedron was formed at 24 h (Fig. 6B). Fig. S3 C, D is the TEM image of the product obtained without the adjunction of PVP at 0.5 and 7 h, respectively. Irregular-shaped CdS aggregates are

obtained in the whole process. From the comparative experiments we can see that in the absence of HMT, smaller particles cannot be able to aggregate into sphere like products, while irregular aggregates are obtained in the presence of HMT, which implies that HMT induced the aggregation of CdS nanocrystallites with sphere-like structure and this supports our deduction about the effect of HMT. On the contrary, we can conclude that PVP deeply influences the sub-crystallites, which suggests that PVP capped or adhered to peculiar surfaces selectively and controlled the growth of CdS nanocrystallites that compose the hollow structures. Fig. S3 E, F reveals the TEM images of the product obtained in the absence of IL at 0.5 and 7 h. We can see that only solid spheres in the diameter of 100 nm were obtained without hollow structures in the whole process. Therefore, IL accelerates the formation of hollow structure. Moreover, solid spheres were formed under the interaction of HMT and PVP, which implies that both PVP and HMT are indispensable.

3.3. Formation mechanism of CdS hollow nanospheres

To understand better the formation mechanism and evolution of the hollow nanostructures, time-dependent experiments with a Cd/S molar ratio of 1:2 were carried out. Fig. 9 shows the morphology evolution process of CdS hollow nanospheres at different reaction time of 0.5, 7, 14 and 20 h. From Fig. 9A, we can see that well dispersed solid spheres of ca. 70–150 nm in diameter with a smooth shell were formed at first. With the extension of reaction time to 7 h, the morphologies changed from solid spheres to incompact solid spheres (70 nm) (Fig. 9B). When the

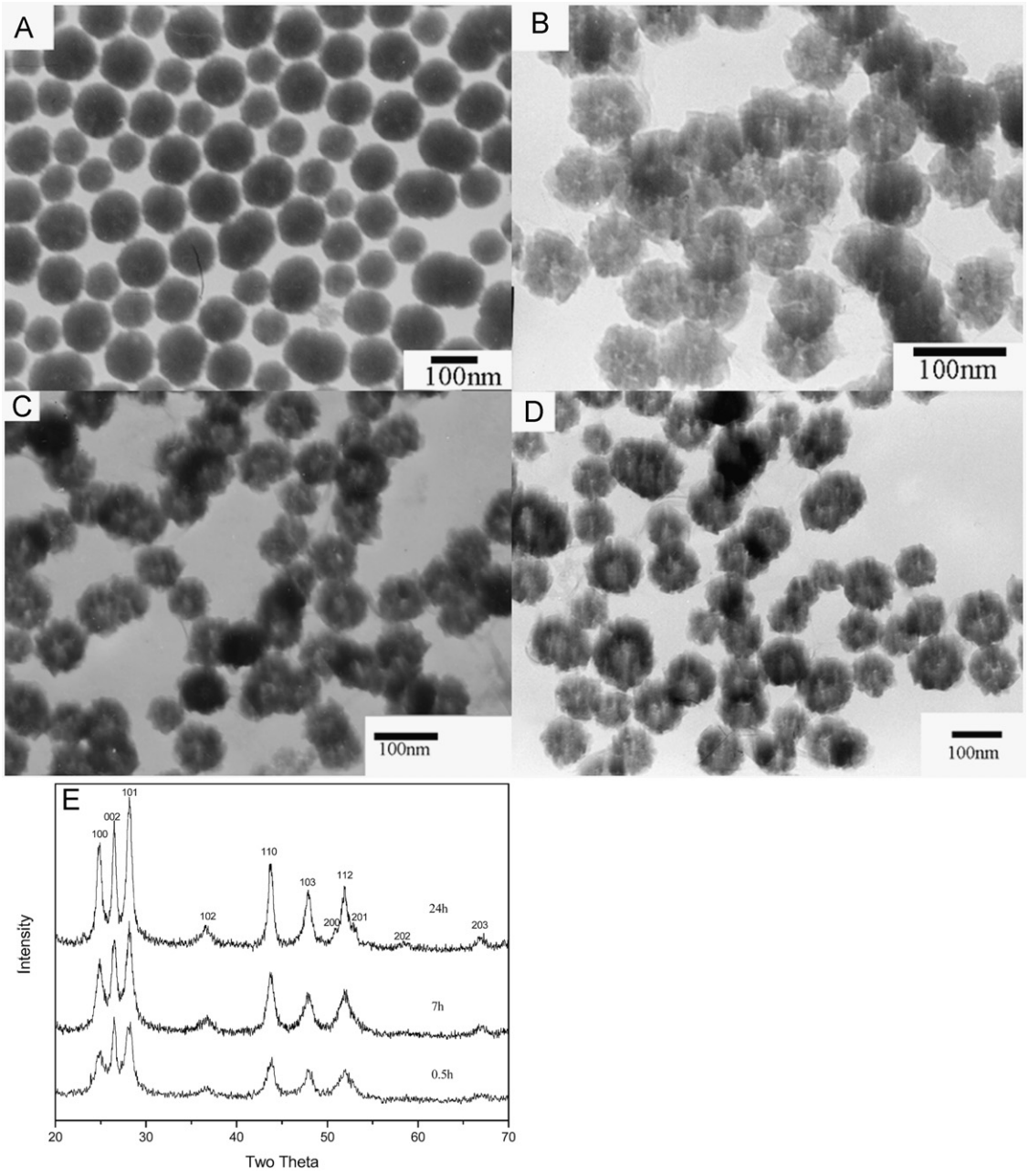

Fig. 9. Shape-evolution processes at different reaction time: (A) 0.5, (B) 7, (C) 14, (D) 20 h and (E) XRD patterns of the samples prepared at different reaction time of 2, 7 and 24 h.

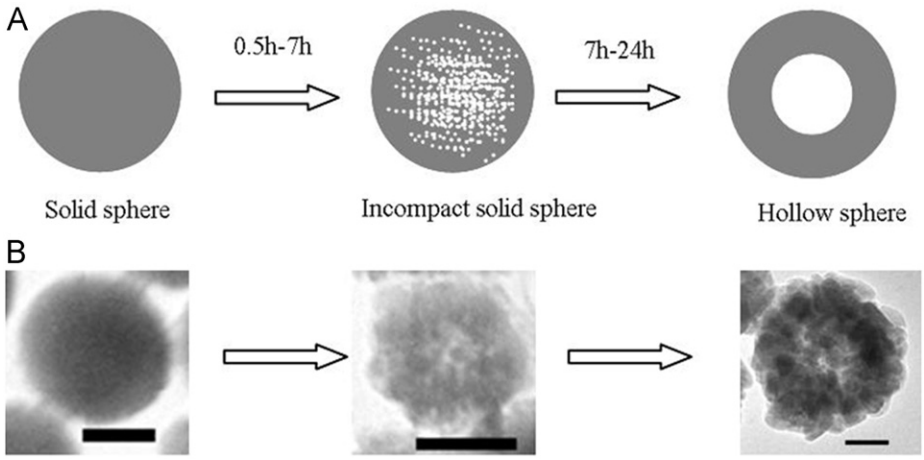

Fig. 10. (A) Schematic illustration of formation mechanism of hollow nanospheres and (B) TEM images of the solid sphere, incompact solid sphere, and hollow sphere obtained at 150 °C after 0.5, 7 and 24 h, respectively. The scale bar represents 50 nm.

reaction time was prolonged to 14 h, hollow nanospheres with an obviously open void can be seen in Fig. 9C, the diameter is about 80 nm. When the reaction time was increased to more than 14 h, the morphology of hollow spheres did not alter obviously except that the diameter slightly increased from ca. 100 nm at 20 h to ca. 130 nm at 24 h. It is obvious that the shells of the products were constructed by small nanocrystallites with their sizes in the approximate range of 20–50 nm. Furthermore, the products were nearly monodispersed with a regular shape. The growth of nanocrystallites in the hollow nanospheres is further demonstrated by XRD results (Fig. 9F), as the peak width becomes narrower and the intensity becomes stronger at longer reaction time, which indicates an Ostwald ripening process (crystallites grow at the expense of the smaller ones) [28].

A plausible mechanism was therefore proposed to address the template-free formation of hollow CdS nanospheres (Fig. 10). A similar mechanism has been used to explain the formation of TiO_2, SnO_2, $CdMO_4$ hollow spheres and CuO/Cu_2O composite hollow microspheres [26,29–31]. Generally, Ostwald ripening involves the formation of aggregates with primary crystallites through a recrystallization process due to the energy difference among them [29,32]. In our work, during the initial stage of the reaction, smaller CdS nanoparticles aggregated together to form solid nanospheres with a loose structure. With prolonged hydrothermal treatment, the inner crystallites of the aggregates went through the mass transfer to the outer shell by a dissolution–recrystallization process at the cost of the small ones, which have higher surface energies and solubility than the larger ones. With the increasing reaction time, outward migration of CdS crystal would result in the continued expansion of interior space, thus, the inner space of the spheres is further increased, which results in the CdS hollow structures. Furthermore, the effect of temperature on the CdS morphology also supports the fact that Ostwald ripening effect is the essential mechanism. It should be mentioned that a similar inside-out evacuation mechanism was also proposed by Lin and Xu for the hydrothermal preparation of CdS hollow nanospheres [18].

3.4. UV–vis, PL and Raman spectrum of the synthesized CdS hollow nanospheres

Further characterizations of as-prepared hollow CdS nanoparticles were performed by UV–vis absorption and PL spectrum. Fig. 11A shows the UV–vis spectrum of as-prepared CdS hollow nanostructures. The absorption peak is at about 482 nm, which shows blue-shifted compared with that of bulk CdS (513 nm) [33]. It indicates the quantum confinement effect.

The room temperature PL spectrum of CdS with 390 nm excitation was shown in Fig. 11B. The broad emission peak centered at 531 nm (2.34 eV), which is assigned to near band emission due to the recombination of excitons and/or shallow trapped electron–hole pairs, respectively, showing the intrinsic character of the CdS hollow nanoparticles [34]. Similar near band emission from CdS nanowires, nanoribbons and 3D nanocrystals was also reported by several groups [25,34–36]. Defect related red emission from trapped states was also reported in CdS nanowires [37]. In the present case, the absence of defect related red emission from the hollow nanospheres demonstrates that the as-prepared CdS hollow nanospheres have excellent optical property and could be used to fabricate photonic devices. Despite the absence of any prominent defect-related PL peaks, the existence of some low intensity peaks just below the band edge could not be ruled out, as the radiative centers are always present surrounding the surface of the hollow nanoparticles due to their high surface to volume ratio.

Raman spectroscopy is a powerful tool for the investigation of lattice defect identification and crystal orientation properties of the materials. Fig. 11C displays the Raman spectrum of the as-prepared CdS hollow nanospheres with characteristic properties analogous to the pure crystalline CdS [35,36]. Two strong and broad peaks located at 292 and 594 cm^{-1} are ascribed to first- (1 LO) and second-longitudinal optical phonon (2 LO) modes of CdS, respectively [38,39]. Compared to the published results [39], the LO peaks are all downshifted and asymmetric broadening, which was probably due to the confinement of optical photons in a hollow CdS nanospheres [40].

3.5. Photocatalytic degradation activity

Fig. 12a reveals the decolorization process of MB in the presence of as-prepared CdS hollow nanospheres. We can see that around 91% of decolorization was achieved at 80 min, and complete decolorization occurred at about 155 min. Furthermore, we noted a continued fading of the coloration of MB solution as a function of reaction time, implying the containable degradation of organic dyes. We also investigated the decolorization process in the

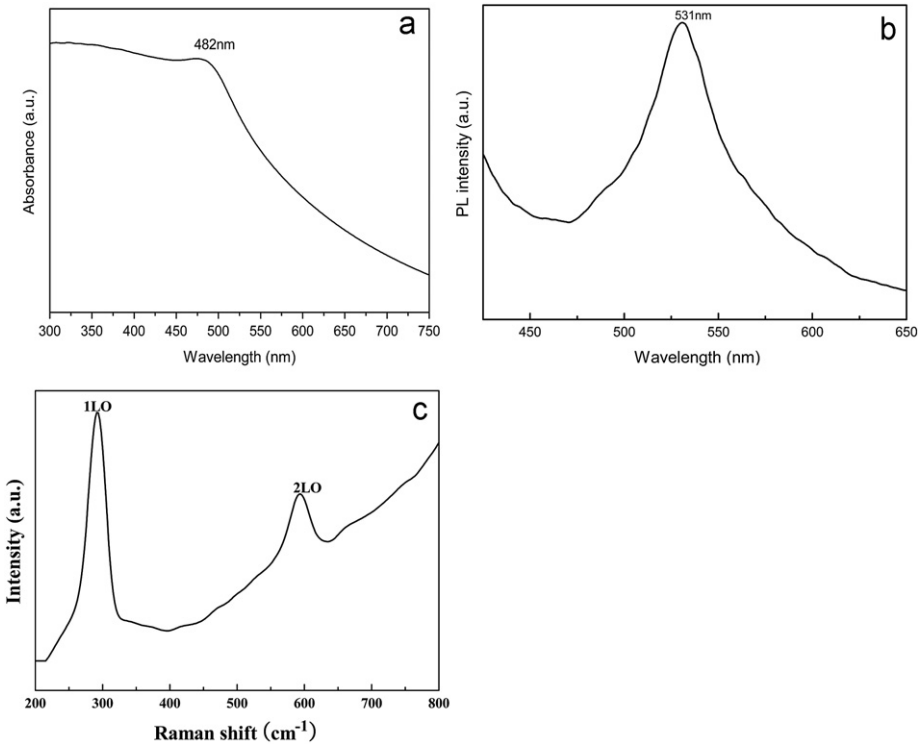

Fig. 11. (A) UV–vis spectrum of CdS hollow nanospheres. (B) Room-temperature photoluminescence (PL) spectrum of the CdS hollow nanospheres. The excitation spectrum was 390 nm. (C) Raman spectrum of CdS hollow nanospheres.

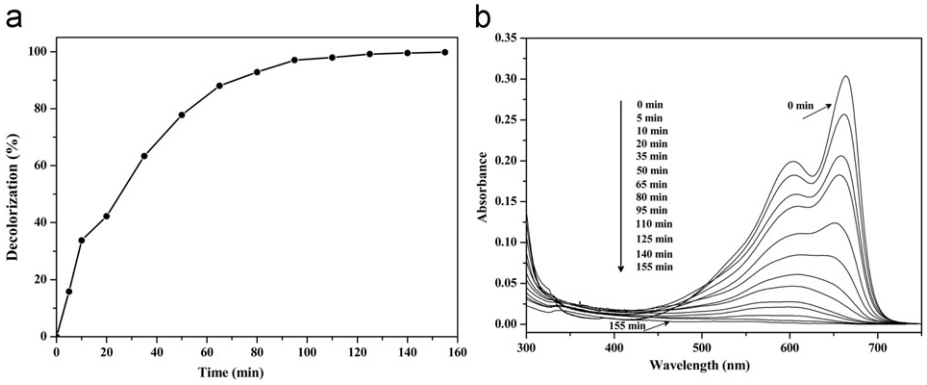

Fig. 12. (a) Photocatalytic degradation of methylene blue in the presence of as-prepared CdS hollow nanospheres; 0.05 g samples were used for the degradation of 200 ml 3×10^{-5} M methylene blue solution. (b) The time-dependent absorption of methylene blue in the presence of the as-prepared CdS hollow nanospheres.

presence of sample but in the dark, which was not showed here, the decolorization efficiency falls a lot and the corresponding data were 22% in 210 min, obviously, the decolorization was not dominated by adsorption but by photocatalytic degradation, which was consistent with Xu's work [18]. Meanwhile, we found that our decolorization efficiency was higher, which may be ascribed to the higher surface area and nanometer hollow structure.

Fig. 12b denotes the time-dependent UV–vis absorbance spectrum of MB during the photocatalytic degradation process in the presence of CdS hollow nanospheres. With the increase of photocatalytic time, the sharp peak at 664 nm gradually diminishes and completely disappears after 155 min, which suggests that the CdS hollow nanospheres are effective catalysts for MB solution degradation.

4. Conclusions

In summary, a template-free ionic liquid (IL) assisted hydrothermal route has been developed to synthesize, in high yield, CdS hollow nanospheres in the presence of polyvinylpyrrolidone (PVP) and hexamethylenetetramine (HMT). Structural characterization by TEM, SEM, SAED and XRD indicates that the CdS hollow nanospheres are polycrystalline consisting of some smaller nanoparticles. The formation of such nanospheres is attributed to the preferential adsorption of PVP molecules on the CdS crystal nuclei. The small crystal nuclei aggregated to form solid nanoparticles that are protected by the adsorption of HMT molecules on certain faces of nanoparticles. The solid nanoparticles experienced a localized Ostwald ripening process and finally the CdS hollow nanospheres are obtained. The reaction

temperature, the molar ratios of Cd/S, the concentration of capping agents (PVP and HMT) and IL [bmim][PF_6] were found to be crucial for the formation of CdS hollow nanospheres. These hollow structured materials can be used as efficient photocatalysts for the degradation of MB. The CdS hollow nanospheres with near band emission, may find promising applications in microelectronic and photovoltaic devices. Importantly, the ionic liquid (IL) assisted hydrothermal route may be a versatile method to prepare hollow nanomaterials, since our studies show that the method is also feasible to prepare Bi_2S_3 hollow nanospheres, which is being under investigation.

Acknowledgment

This work was supported by the National Natural Science Foundation of China (no's. 20773081, 50972080), National Basic Research Program (2007CB808004, 2009CB930101), and Laboratory of Organic Optoelectronic Functional Materials and Molecular Engineering, TIPC, CAS.

Appendix. Supplementary material

Supplementary data associated with this article can be found in the online version at doi:10.1016/j.jssc.2010.04.001.

References

[1] C.G. Goltner, Angew. Chem. Int. Ed. 38 (1999) 3155–3156.
[2] F. Caruso, R.A. Caruso, H. Mihwald, Science 282 (1998) 1111–1114.
[3] X.W. Lou, L.A. Archer, Z.C. Chao, Adv. Mater. 20 (2008) 3987–4019.
[4] Y.R. Ma, L.M. Qi, J. Colloid Interface Sci. 335 (2009) 1–10.
[5] J. Goldberger, R. He, S. Lee, Y. Zhang, H. Yan, H. Choi, P. Yang, Nature 422 (2003) 599–602.
[6] T. Nakashima, N. Kimizuka, J. Am. Chem. Soc. 125 (2003) 6386–6387.
[7] G.Z. Chen, C.X. Xu, X.Y. Song, S.L. Xu, Y. Ding, S.X. Sun, Cryst. Growth Des. 8 (2008) 4449–4453.
[8] W.J. Lou, M. Chen, X.B.W.M. Wang, Chem. Mater. 19 (2007) 872–878.
[9] X. Cao, L. Gu, L. Zhuge, W. Gao, W. Wang, S. Wu, Adv. Funct. Mater. 16 (2006) 896–902.
[10] S. Acharya, I. Patla, J. Kost, S. Efrima, Y. Golan, J. Am. Chem. Soc. 128 (2006) 9294–9295.
[11] X. Fan, M.L. Zhang, I. Shafiq, W.J. Zhang, C.S. Lee, S.T. Lee, Cryst. Growth Des. 9 (2009) 1375–1377.
[12] P.C. Wu, R.M. Ma, C. Liu, T. Sun, Y. Ye, L. Dai, J. Mater. Chem. 19 (2009) 2125–2130.
[13] M.H. Chen, Y.N. Kim, C.C. Li, S.O. Cho, Cryst. Growth Des. 8 (2008) 629–634.
[14] Y. Xie, J.X. Huang, B. Li, Y. Liu, Y.T. Qian, Adv. Mater. 12 (2000) 1523–1526.
[15] Q. Gong, X.F. Qian, P.L. Zhou, X.B. Yu, W.M. Du, S.H. Xu, J. Phys. Chem. C 111 (2007) 1935–1940.
[16] M.R. Kim, D.J. Jang, Chem. Commun. (2008) 5218.
[17] Y.R. Ma, L.M. Qi, J.M. Ma, H.M. Cheng, W. Shen, Langmuir 19 (2003) 9079–9085.
[18] G.F. Lin, J.W. Zheng, R. Xu, J. Phys. Chem. C 112 (2008) 7363–7370.
[19] R.R. Deshmukh, R. Rajagopal, K.V. Srinivasan, Chem. Commun. (2001) 1544–1545.
[20] Y. Wang, H. Yang, J. Am. Chem. Soc. 127 (2005) 5316–5317.
[21] J.G. Huddleston, H.D. Willauer, R.P. Swatloski, A.E. Visser, R.D. Rogers, Chem. Commun. (1998) 1765–1766.
[22] P.T. Zhao, K.X. Huang, Cryst. Growth Des. 8 (2008) 717–722.
[23] Y.H. Tong, Y.C. Liu, L. Dong, D.X. Zhao, J.Y. Zhang, Y.M. Lu, D.Z. Shen, X.W. Fan, J. Phys. Chem. B 110 (2006) 20263–20267.
[24] X.G. Peng, L. Manna, W.D. Yang, J. Wickham, E. Scher, A. Kadavanich, A.P. Alivisatos, Nature 404 (2000) 59–61.
[25] F. Chen, R.J. Zhou, L.G. Yang, N. Liu, M. Wang, H.Z. Chen, J. Phys. Chem. C 112 (2008) 1001–1007.
[26] X.W. Lou, Y. Wang, C. Yuan, J.Y. Lee, L.A. Archer, Adv. Mater. 18 (2006) 2325–2329.
[27] X.W. Lou, L.A. Archer, Z.C. Yang, Adv. Mater. 20 (2008) 1853–1858.
[28] W.Z. Ostwald, Phys. Chem. 34 (1900) 495.
[29] H.G. Yang, H.C. Zeng, J. Phys. Chem. B 108 (2004) 3492–3495.
[30] W.S. Wang, L. Zhen, C.Y. Xu, B.Y. Zhang, W.Z. Shao, J. Phys. Chem. B 110 (2006) 23154–23158.
[31] H.G. Yu, J.G. Yu, S.W. Liu, S. Mann, Chem. Mater. 19 (2007) 4327–4334.
[32] P. Hu, L.J. Ye, A. Zuo, C.Y. Guo, F. Yuan, J. Phys. Chem. C 113 (2009) 900–906.
[33] H. Weller, Angew. Chem. Int. Ed. 32 (1993) 41–53.
[34] Z.H. Dai, J. Zhang, J.C. Bao, X.H. Huang, X.Y. Mo, J. Mater. Chem. 17 (2007) 1087–1093.
[35] S. Kar, B. Satpati, P.V. Satyam, S. Chaudhuri, J. Phys. Chem. B 109 (2005) 19134–19138.
[36] Y.K. Liu, J.A. Zapien, C.Y. Geng, Y.Y. Shan, C.S. Lee, S.T. Lee, Appl. Phys. Lett. 85 (2004) 3241–3243.
[37] Y. Wang, G. Meng, L. Zhang, C. Liang, J. Zhang, Chem. Mater. 14 (2002) 1773–1777.
[38] R.C.C. Leite, S.P.S. Porto, Phys. Rev. Lett. 17 (1966) 1012.
[39] J.S. Suh, J.S. Lee, Chem. Phys. Lett. 281 (1997) 384–388.
[40] B.L. Cao, Y. Jiang, C. Wang, W.H. Wang, L.Z. Wang, M. Niu, W.J. Zhang, Y.Q. Li, S.-T. Lee, Adv. Funct. Mater. 17 (2007) 1501–1506.